Kinetics and Mechanism of RNA Binding by Triplex Tethered Oligonucleotide Probes

Arikha C. Moses and Alanna Schepartz*

Contribution from the Department of Chemistry, Yale University, P.O. Box 208107, New Haven, Connecticut 06520-8107

Received May 6, 1997[⊗]

Abstract: We have described a series of tethered oligonucleotide probes (triplex TOPs) that recognize one single-stranded and one double-stranded region of an RNA simultaneously through the formation of Watson−Crick and Hoogsteen base pairs, respectively. Here we describe studies on the kinetics and mechanism of triplex TOP·RRE^{AU} association and dissociation. Because triplex TOP·RRE^{AU} complexes cannot be observed by direct electrophoretic methods, kinetics was monitored by use of a competitive electrophoretic mobility shift assay that quantified the effect of a triplex TOP on the association and dissociation rates of an electrophoretically stable TOP·RRE^{AU} complex. Association and dissociation rate constants of triplex TOP·RRE^{AU} complexes were extracted from the experimental data by numerical integration. Triplex TOP·RRE^{AU} association reactions at 25 °C were characterized by rate constants between $(7.8 \pm 2.0) \times 10^3$ and $(16 \pm 3) \times 10^3$ M^{-1} s^{-1}, while dissociation reactions were characterized by rate constants between $(3.3 \pm 1.0) \times 10^{-4}$ and $(5.4 \pm 2.0) \times 10^{-2}$ s^{-1}. Rate constants for association of triplex TOP·RRE^{AU} complexes were insensitive to the length and sequence of the 3′-oligonucleotide that mediates triple helix formation. Rate constants for dissociation of triplex TOP·RRE^{AU} complexes were sensitive to changes in tether length as well as the length and composition of the 3′-oligonucleotide. Taken together, these data suggest that triplex TOPs follow a kinetic pathway for binding RRE^{AU} in which duplex formation is rate-limiting and precedes triple helix formation. The implication of our data with regard to the kinetics of triple helix association within the context of a highly structured RNA is discussed.

Large, structured RNA molecules play critical roles in cellular and viral life cycles.[1−3] A considerable body of biochemical structure-mapping data,[4−6] along with several high-resolution structures,[7−15] indicate that many large RNAs are composed of irregular arrangements of short single- and double-stranded regions joined by structures such as loops, bulges, and pseudoknots.[16−19] These irregular architectures present complex functional group arrays that are recognized in nature by proteins,[20−23] other nucleic acids,[2,24] and small organic molecules.[25] There is considerable current interest in the design of molecules that mimic the properties of these natural ligands, not only to inhibit the translation of messenger RNAs but also to interrupt the functions of catalytic and regulatory RNAs.[26−32]

Several strategies have been presented for the recognition of large, structured RNA molecules. Ribozymes and single-stranded oligonucleotides[33−35] recognize RNA on the basis of primary sequence.[36−40] Although a strategy based on primary sequence recognition is broadly applicable in theory, it requires a target sequence that is unique, accessible, and single-stranded.[41−47] These requirements can be difficult to fulfill in practice.

* Corresponding author. Phone: 203-432-5094. Fax: 203-432-6144. E-mail: alanna@milan.chem.yale.edu.

⊗ Abstract published in *Advance ACS Abstracts,* October 15, 1997.

(1) Standart, N.; Jackson, R. J. *Biochimie* **1994,** *76,* 867.

(2) *The RNA World*; Cold Spring Harbor Press: Cold Spring Harbor, NY, 1993.

(3) Pain, V. M. *Eur. J. Biochem.* **1996,** *236,* 747.

(4) Peattie, D. A.; Gilbert, W. *Proc. Natl. Acad. Sci. U.S.A.* **1980,** *77,* 4679.

(5) Ehresmann, C.; Baudin, F.; Mougel, M.; Romby, P.; Ebel, J. P.; Ehresmann, B. *Nucleic Acids Res.* **1987,** *15,* 9109.

(6) Huber, P. W. *FASEB J.* **1993,** *7,* 1367.

(7) Jack, A.; Ladner, J. E.; Klug, A. *J. Mol. Biol.* **1976,** *108,* 619.

(8) Schevitz, R. W.; Podjarny, A. D.; Krishnamachari, N.; Hughes, J. J.; Sigler, P. B. *Nature* **1979,** *278,* 188.

(9) Basavappa, R.; Sigler, P. B. *EMBO J.* **1991,** *10,* 3105.

(10) Cate, J. H.; Gooding, A. R.; Podell, E.; Zhou, K.; Golden, B. L.; Kundrot, C. E.; Cech, T. R.; Doudna, J. A. *Science* **1996,** *273,* 1678.

(11) Scott, W. G.; Murray, J. B.; Arnold, J. R. P.; Stoddard, B.; Klug, A. *Science* **1996,** *274,* 2065.

(12) Cate, J. H.; Doudna, J. A. *Structure* **1996,** *4,* 1221.

(13) Cate, J. H.; Gooding, A. R.; Podell, E.; Zhou, K.; Golden, B. L.; Szewczak, A. A.; Kundrot, C. E.; Cech, T. R.; Doudna, J. A. *Science* **1996,** *273,* 1696.

(14) Pley, H. W.; Flaherty, K. M.; McKay, D. B. *Nature* **1994,** *372,* 111.

(15) Pley, H.; Flaherty, K.; McKay, D. *Nature* **1994,** *372,* 111.

(16) Tinoco, I. J.; Davis, P. W.; Hardin, C. C.; Puglisi, J. D.; Walker, G. T.; Wyatt, J. *Cold Spring Harbor Symp. Quant. Biol.* **1987,** *52,* 135.

(17) Tinoco, I. J.; Puglisi, J. D.; Wyatt, J. R. *Nucleic Acids Mol. Biol.* **1990,** *4,* 205.

(18) Chastain, M.; Tinoco, I. J. *Prog. Nucleic Acid Res. Mol. Biol.* **1991,** *41,* 131.

(19) Dam, E. T.; Pleij, K.; Draper, D. *Biochemistry* **1992,** *31,* 11665.

(20) Frankel, A. D.; Mattaj, I. W.; Rio, D. C. *Cell* **1991,** *67,* 1041.

(21) Mattaj, I. W. *Cell* **1993,** *73,* 837.

(22) Burd, C. G.; Dreyfuss, G. *Science* **1994,** *265,* 615.

(23) Draper, D. E. *Annu. Rev. Biochem.* **1995,** *64,* 593.

(24) *Ribosomal RNA and Group I Introns*; R. G. Landes: Austin, TX, 1996; Vol. 1.

(25) Bass, B. L.; Cech, T. R. *Nature* **1984,** *308,* 820.

(26) Stephenson, M. L.; Zamecnik, P. C. *Proc. Natl. Acad. Sci. U.S.A.* **1978,** *75,* 285.

(27) Ahsen, U. v.; Davies, J.; Schroeder, R. *Nature* **1991,** *353,* 368.

(28) Renneisen, K.; Leserman, L.; Mattes, E.; Schroder, H. C.; Muller, W. E. G. *J. Biol. Chem.* **1990,** *265,* 16337.

(29) Li, G.; Lisziewicz, J.; Sun, D.; Zon, G.; Daefler, S.; Wong-Staal, F.; Gallo, R. C.; Klotman, M. E. *J. Virol.* **1993,** *67,* 6882.

(30) Zapp, M. L.; Stern, S.; Green, M. R. *Cell* **1993,** *74,* 969.

(31) Stage, T. K.; Hertel, K. J.; Uhlenbeck, O. C. *RNA* **1995,** *1,* 95.

(32) Ratmeyer, L.; Zapp, M. L.; Green, M. R.; Vinayak, R.; Kumar, A.; Boykin, D. W.; Wilson, W. D. *Biochemistry* **1996,** *35,* 13689.

(33) Burke, J. M.; Erzal-Herranz, A. *FASEB J.* **1993,** *7,* 106.

(34) *Antisense oligodeoxynucleotides and antisense RNA: Novel pharmacological and therapeutic agents*; Weiss, B., Ed.; CRC Press: Boca Raton, FL, 1997.

(35) Bartel, D. P.; Szostak, J. W. *Science* **1993,** *261,* 1411.

(36) Gold, L.; Polisky, B.; Uhlenbeck, O.; Yarus, M. *Annu. Rev. Biochem.* **1995,** *64,* 763.

(37) Mesmaeker, A. D.; Häner, R.; Martin, P.; Moser, H. E. *Acc. Chem. Res.* **1995,** *28,* 366.

(38) Sharma, H. W.; Narayanan, R. *Bioessays* **1995,** *17,* 1055.

(39) Egli, M. *Angew. Chem., Int. Ed. Engl.* **1996,** *35,* 1894.

(40) Stein, C. A.; Cheng, Y.-C. *Science* **1993,** *261,* 1004.
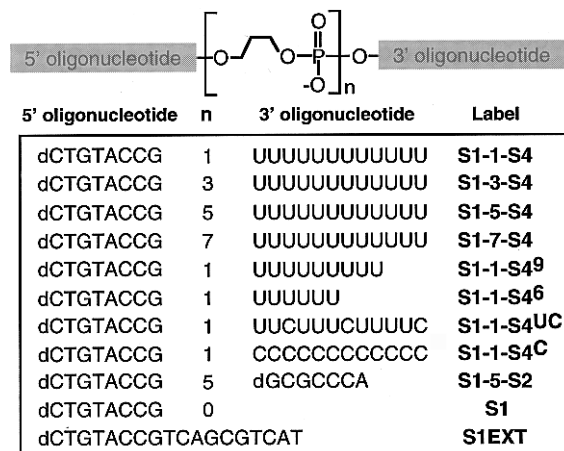
Figure 1. Sequences of TOPs and oligonucleotides used in this study.

Organometallic complexes and small organic molecules recognize more irregular elements of structure. For example, various rhodium complexes recognize expanded RNA major grooves[48,49] or G·U mismatches,[50] and the organometallic complexes methidiumpropyl-EDTA and bis(phenanthroline)copper(II) show some preference for junctions between duplexes and single-stranded loops or bulges.[51,52] The aminoglycoside antibiotic neomycin B recognizes a distinct stem−loop structure within the group I ribozyme,[53] the hammerhead enzyme−substrate complex,[31] the Rev response element RNA,[54] and, under certain conditions, 16S rRNA.[55,56] Although combinatorial methods may prove extremely useful for identifying small molecule ligands for specific RNAs,[57] few general strategies exist for the design of molecules capable of binding large, globular RNAs in a sequence- and structure-dependent fashion.

Several years ago our laboratory presented a general strategy through which the structure and sequence of an RNA might be recognized (Figure 1).[47,58−62] Our strategy is based on a class of molecules called tethered oligonucleotide probes (TOPs). A TOP consists of two short oligonucleotides joined by a tether whose length and composition may be varied using chemical synthesis. Each of the oligonucleotides within a TOP recognizes a single, accessible sequence within the target RNA, and the

(41) Uhlenbeck, O. C. *J. Mol. Biol.* **1972**, *65*, 25.
(42) Freier, S. M.; Tinoco, I. J. *Biochemistry* **1975**, *14*, 3310.
(43) Freier, S. M.; Lima, W. F.; Sanghvi, Y. S.; Vickers, T.; Zounes, M.; Cook, P. D.; Ecker, D. J. *Raven Press Ser. Mol. Cell. Biol.* **1992**, *1*, 95.
(44) Rittner, K.; Burmester, C.; Sczakiel, G. *Nucleic Acids Res.* **1993**, *21*, 1381.
(45) Homann, M.; Rittner, K.; Sczakiel, G. *J. Mol. Biol.* **1993**, *233*, 7.
(46) Kronenwett, R.; Haas, R.; Sczakiel, G. *J. Mol. Biol.* **1996**, *259*, 632.
(47) Cload, S. T.; Schepartz, A. *J. Am. Chem. Soc.* **1994**, *116*, 437.
(48) Chow, C. S.; Barton, J. K. *J. Am. Chem. Soc.* **1990**, *112*, 2839.
(49) Chow, C. S.; Behlen, L. S.; Uhlenbeck, O. C.; Barton, J. K. *Biochemistry* **1992**, *31*, 972.
(50) Chow, C. S.; Barton, J. K. *Biochemistry* **1992**, *31*, 5423.
(51) Kean, J. M.; White, S. A.; Draper, D. E. *Biochemistry* **1985**, *24*, 5062.
(52) Murakawa, G. J.; Chem, C.-h., B.; Kuwabare, M. D.; Nierlich, D. P.; Sigman, D. S. *Nucleic Acids Res.* **1989**, *17*, 5361.
(53) von Ahsen, U.; Noller, H. F. *Science* **1993**, *260*, 1500.
(54) Werstuck, G.; Zapp, M. L.; Green, M. R. *Chem. Biol.* **1996**, *3*, 129.
(55) Moazed, D.; Noller, H. F. *Nature (London)* **1987**, *327*, 389.
(56) Famulok, M.; Huttenhofer, A. *Biochemistry* **1996**, *35*, 4265.
(57) Park, W. K. C.; Auer, M.; Jaksche, H.; Wong, C.-H. *J. Am. Chem. Soc.* **1996**, *118*, 10150.
(58) Richardson, P. L.; Schepartz, A. *J. Am. Chem. Soc.* **1991**, *113*, 5109.
(59) Cload, S. T.; Schepartz, A. *J. Am. Chem. Soc.* **1991**, *113*, 6324.
(60) Cload, S. T.; Richardson, P. L.; Huang, Y.-H.; Schepartz, A. *J. Am. Chem. Soc.* **1993**, *115*, 5005.
(61) Moses, A.; Schepartz, A. *J. Am. Chem. Soc.* **1996**, *118*, 10896.
(62) Moses, A. C.; Huang, S.; Schepartz, A. *Bioorg. Med. Chem.* **1997**, *5*, 1123.
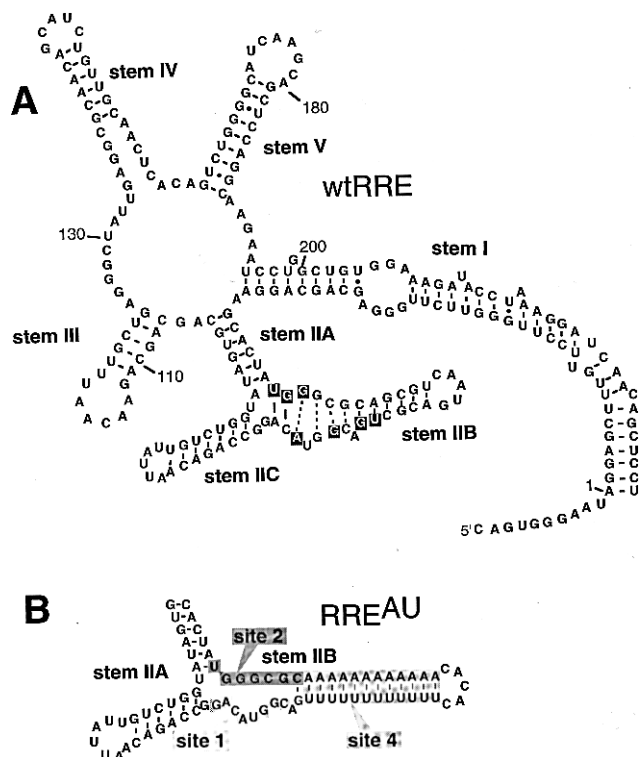
Figure 2. Sequences of (A) wild type RRE (wtRRE) and (B) RRE^{AU}. Those residues within wtRRE that contact Rev directly[85,86] are shaded, as are sites 1, 2, and 4 of RRE^{AU}. RRE^{AU} is numbered in accord with wtRRE.

tether traverses the distance between the two sequences. In contrast to traditional oligonucleotides which recognize a single, contiguous RNA sequence, TOPs recognize two short, noncontiguous sequences that are proximal in the folded RNA. Because TOPs bind simultaneously to two accessible sequences, rather than one long sequence that may not be fully accessible, TOPs exhibit very high affinities for structured RNA targets and bind these targets more rapidly than molecules that must disrupt structure in order to bind.[47,60]

Initially, we evaluated TOPs that recognized two noncontiguous single-stranded sequences within a target RNA through the formation of standard Watson−Crick base pairs.[47,58−60] More recently, we evaluated TOPs that recognized one single-stranded and one double-stranded region simultaneously through the formation of Watson−Crick and Hoogsteen base pairs, respectively.[61,62] These molecules were termed triplex TOPs. The RNA target for our triplex TOPs was a modified version of the HIV-1 Rev response element (RRE) (Figure 2A) in which twelve contiguous A-U base pairs replaced a portion of stem−loop IIB (RRE^{AU}, Figure 2B). The 5′-oligonucleotide within each triplex TOP recognized the accessible, single-stranded region between positions 69 and 76 of RRE^{AU} (site 1) to form a duplex and the 3′-oligonucleotide recognized the AU-rich duplex (site 4) to form a triple helix. Triplex TOPs designed to recognize RRE^{AU} sites 1 and 4 formed complexes with nanomolar dissociation constants[61] and were effective inhibitors of Rev·RRE^{AU} complexation at equilibrium *in vitro*.[62]

Here we characterize the kinetics and mechanism of triplex TOP·RRE^{AU} association and dissociation. Because triplex TOP·RRE^{AU} complexes cannot be observed by direct electrophoretic methods,[61] kinetics was monitored by use of a competitive electrophoretic mobility shift assay[63−65] that quanti-

(63) Aranyi, P. *Biochim. Biophys. Acta* **1980**, *628*, 220.
(64) Kim, J. G.; Takeda, Y.; Matthews, B. W.; Anderson, W. F. *J. Mol. Biol.* **1987**, *196*, 149.
(65) Gerstle, J. T.; Fried, M. G. *Electrophoresis* **1993**, *14*, 725.

fied the effect of a triplex TOP on the association and dissociation rates of a electrophoretically stable TOP·RRE^{AU} complex.[47] Association and dissociation rate constants were extracted from the experimental data by numerical integration. Triplex TOP·RRE^{AU} association reactions were characterized by rate constants between $(7.8 \pm 2.0) \times 10^3$ and $(16 \pm 3) \times 10^3$ M^{-1} s^{-1} at 25 °C, while dissociation reactions were characterized by rate constants between $(3 \pm 1) \times 10^{-4}$ and $(400 \pm 40) \times 10^{-4}$ s^{-1}. Association rate constants were insensitive to changes in the length and sequence of the 3′-oligonucleotide that mediates triple-helix formation, whereas dissociation rate constants were sensitive to changes in 3′-oligonucleotide sequence and length as well as changes in tether length. Taken together, these data indicate that triplex TOPs bind RRE^{AU} through a kinetic pathway in which duplex formation is rate-limiting and precedes triple-helix formation.

Experimental Section

Synthesis of Tethered Oligonucleotide Probes. TOPs and oligonucleotides were synthesized on a 1 μmol scale[58,61] by use of the solid-phase phosphoramidite method[66] on a Perseptive Biosystems model 8909 nucleic acid synthesizer. Oligonucleotides S1 and S1EXT and TOP S1-5-S2 were cleaved from the solid support and deprotected upon treatment with 12 M NH$_4$OH at 55 °C for 10 h.[67] All other TOPs were deprotected with ammonia-saturated ethanol at 55 °C for 10 h[68] followed by 1 M tetra-N-butylammonium fluoride (TBAF) in THF at 25 °C for 1 h.[69] TOPs and oligonucleotides were purified by use of denaturing polyacrylamide gel electrophoresis (20% acrylamide, 19:1 acrylamide:N,N'-methylenebis(acrylamide), 7 M urea).[70] TOPs were stored in diethyl pyrocarbonate-treated (DEPC) water[71,72] at −20 °C and thawed prior to use. S1-5-S2 was labeled on the 5′-end by use of [γ-^{32}P]ATP and T4 polynucleotide kinase.[70]

Preparation of RRE^{AU}. RRE^{AU} was prepared by use of T7 RNA polymerase[73] (Promega) and a chemically synthesized DNA template. RRE^{AU} was purified by preparative denaturing gel electrophoresis (20% acrylamide, 19:1 acrylamide:N,N'-methylenebis(acrylamide), 7 M urea) and desalted prior to use in kinetic experiments. The sequence of the 5′ 52 residues of RRE^{AU} was confirmed by enzymatic methods[6,74] using protocols recommended by the supplier (Pharmacia). Aliquoted RNA stock solutions were stored in DEPC water[71,72] at −20 °C and thawed prior to use.

Kinetic Analysis: General Procedures. All reactions were performed at 25 °C in binding buffer (10 mM 1,4-piperazinebis-(ethanesulfonate) (Research Organics, Inc.) (pH 7.0), 300 mM NaCl, 2 mM Hepes (pH 7.5), and 10% glycerol). RRE^{AU} (125 nM−1.25 μM) in RRE buffer (5 mM Hepes (pH 7.5), 25 mM NaCl) was renatured before each reaction by heating at 85 °C for 2 min and cooling at 25 °C for 10 min. Binding reactions were analyzed with nondenaturing gels (6% acrylamide, 79:1 acrylamide:N,N'-methylenebis(acrylamide)) prepared with running buffer (20 mM Tris·borate (pH 7.0)). Gels were maintained between 2 and 6 °C during electrophoresis by immersion in a buffer cooled by a circulating temperature-controlled water bath. The fraction of [^{32}P]S1-5-S2 bound to RRE^{AU} was determined by use of a Molecular Dynamics Storm Phosphorimager and ImageQuant

Table 1. Kinetic and Equilibrium Constants for Triplex TOP·RRE^{AU} Complexes at 25 °C[a]

TOP or oligonucleotide	$10^{-3} \times k_2$ (M^{-1} s^{-1})[b]	$10^4 \times k_{-2}$ (s^{-1})	K_d (nM) calcd[c]	K_d (nM) exptl[d]
S1-5-S2	7.8 ± 2.0	4 ± 0.5[b]	51 ± 5	68 ± 8
S1	7.8 ± 2.0	500 ± 200	7000 ± 3000	17700 ± 3500
S1-1-S4	16 ± 3	3 ± 1	21 ± 5	93 ± 15
S1-3-S4	9.5 ± 0.8	29 ± 9	300 ± 150	ND
S1-5-S4	7.8 ± 2.0	28 ± 10	363 ± 160	ND
S1-7-S4	7.8 ± 2.0	120 ± 40	1540 ± 500	ND
S1-1-S4[9]	7.8 ± 2.0	19 ± 10	240 ± 160	814 ± 200
S1-1-S4[6]	7.8 ± 2.0	60 ± 30	810 ± 400	5300 ± 1800
S1-1-S4^{UC}	7.8 ± 2.0	400 ± 40	5130 ± 500	30900 ± 3700
S1-1-S4^C	9.5 ± 2.0	64 ± 30	400 ± 170	1850 ± 380
S1EXT	7.8 ± 2.0	240 ± 70	4200 ± 800	ND

[a] Experimental protocols described in text. [b] This error represents the range of values that provided a good fit (residual less than 5%) to the experimental data. [c] Calculated from the ratio k_{-2}/k_2. [d] Determined by competitive equilibrium mobility shift analysis.[61,62]

software (Molecular Dynamics, Sunnyvale, CA) and was plotted as a function of time using Kaleidagraph v. 3.0.2.

Association and Dissociation Kinetics of [^{32}P]S1-5-S2·RRE^{AU}: Direct Method. In order to verify the accuracy of the competitive kinetic analysis, we measured the rate constants for association and dissociation of the [^{32}P]S1-5-S2·RRE^{AU} complex by direct electrophoretic methods[60,75,76] and compared these values to those obtained by competition and numerical analysis (Table 1). For association reactions, 0.01 nM [^{32}P]S1-5-S2 was added to 30−500 nM RRE^{AU} in binding buffer at 25 °C and aliquots were applied at 2 min intervals to running gels. For dissociation reactions, 50−400 nM RRE^{AU} and 0.01 nM [^{32}P]S1-5-S2 were equilibrated in binding buffer for 90 min at 25 °C. Dissociation was initiated by addition of 10 nM unlabeled S1-5-S2, and aliquots were applied at 30 s intervals to running gels. Data were analyzed as described previously.[60] Association and dissociation reactions were performed at least twice at each RRE^{AU} concentration. Figure 3A illustrates the fraction of [^{32}P]S1-5-S2 bound to RRE^{AU} as a function of time at RRE^{AU} concentrations of 30, 50, 100, 150, 200, and 500 nM. Figure 3B shows the first-order plots that were used to obtain k_{obs}. A value for k_1 of $(7.8 \pm 2.0) \times 10^3$ M^{-1} s^{-1} ($R = 0.98$) was obtained from the slope of the plot of k_{obs} versus [RRE^{AU}] in Figure 3C. This value was identical to the value determined by the competitive method. The intercept at [RRE^{AU}] = 0 in Figure 3C is equal to k_{-1} = $(2.4 \pm 0.5) \times 10^{-4}$ s^{-1}. This value was 2-fold higher than the value for k_{-1} of $(0.93 \pm 0.3) \times 10^{-4}$ s^{-1}; open symbol at [RRE^{AU}] = 0 was determined in independent dissociation experiments and is 2-fold lower than the value determined by the competitive method (see below), $(4.0 \pm 0.5) \times 10^{-4}$ s^{-1} (Figure 3D). The similarity between the kinetic constants for [^{32}P]S1-5-S2·RRE^{AU} association and dissociation determined by the direct and indirect methods validates use of the competitive method to determine kinetic constants for triplex TOP·RRE^{AU} complexes.

Association and Dissociation kinetics of TOP·RRE^{AU} Complexes: Competitive Method. Rate constants describing the association and dissociation of TOP·RRE^{AU} complexes and the S1·RRE^{AU} and S1EXT·RRE^{AU} complexes were determined by use of a competitive electrophoretic mobility shift assay[63−65] in which the fraction of [^{32}P]-S1-5-S2 bound to RRE^{AU} in the presence of varying concentrations of competitor (TOP, S1, or S1EXT) was monitored as a function of time. Our experimental protocol was as follows: RRE^{AU} (250 nM or 1 mM in RRE buffer) was renatured as described above and equilibrated with [^{32}P]S1-5-S2 in binding buffer for 1 h at 25 °C. The concentration of RRE^{AU} (100 or 400 nM final concentration) was chosen such that the fraction of [^{32}P]S1-5-S2 bound to RRE^{AU} was between 0.7 and 0.9 prior to addition of competitor. Dissociation of the [^{32}P]S1-5-S2·RRE^{AU} complex was initiated upon addition of between 500 nM and 15 mM competitor TOP or oligonucleotide, and aliquots of the reaction mixture were applied at 5 min intervals to running gels. Final concentrations were as follows: 0.01 nM [^{32}P]S1-5-S2, 100 or 400 nM RRE^{AU}, 500

(66) Beaucage, S. L.; Caruthers, M. H. *Tetrahedron Lett.* **1981**, *22*, 1859.

(67) Useman, N.; Ogilvie, K. K.; Jiang, M. Y.; Cedergren, R. J. *J. Am. Chem. Soc.* **1987**, *109*, 7845.

(68) Scaringe, S. A.; Francklyn, C.; Usman, N. *Nucleic Acids Res.* **1990**, *18*, 5433.

(69) Hogrefe, R. I.; McCaffrey, A. P.; Borozdina, L. U.; McCampbell, E. S.; Vaghefi, M. M. *Nucleic Acids Res.* **1993**, *21*, 4739.

(70) Maniatis, T.; Fritsch, E. F.; Sambrook, J. *Molecular Cloning: A Laboratory Manual*, 2nd ed.; Cold Spring Harbor Press: Cold Spring Harbor, NY, 1987.

(71) Fedorscak, I.; Ehrenberg, L. *Acta Chem. Scand.* **1966**, *20*, 107.

(72) Kumar, A.; Lindberg, U. *Proc. Natl. Acad. Sci. U.S.A.* **1972**, *69*, 681.

(73) Milligan, J. F.; Groebe, D. R.; Witherell, G. W.; Uhlenbeck, O. C. *Nucleic Acids Res.* **1987**, *15*, 8783.

(74) Hostomsky, Z.; Hostomska, Z.; Matthews, D. A. *Nucleases*; Cold Spring Harbor Laboratory: Cold Spring Harbor, NY, 1993.

(75) Fried, M.; Crothers, D. M. *Nucleic Acids Res.* **1981**, *9*, 6505.

(76) Garner, M. M.; Revzin, A. *Nucleic Acids Res.* **1981**, *9*, 3047.
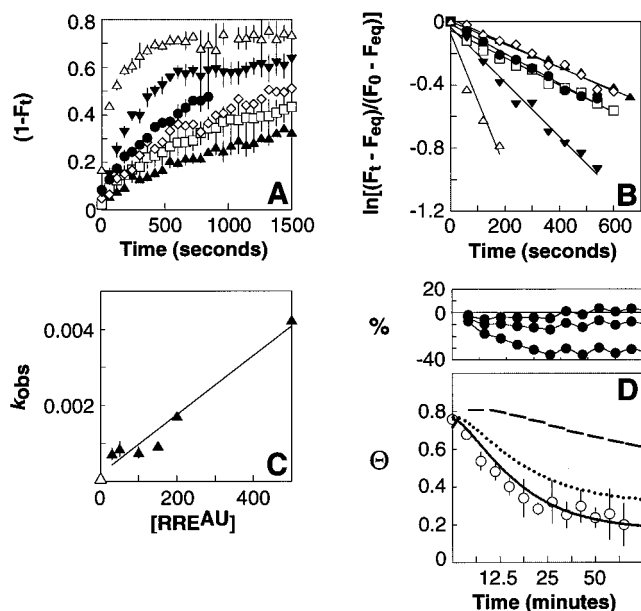
Figure 3. Determination of the rate constant for association of the [^{32}P]S1-5-S2·RRE^{AU} complex by direct and competitive electrophoretic mobility shift analyses. (A) Plot of $(1 - F_t)$, the fraction [^{32}P]S1-5-S2 bound as a function of time, t, in the presence of [RRE^{AU}] = ▲, 30 nM; □, 50 nM; ◇, 100 nM; ●, 150 nM; ▼, 200 nM; △, 500 nM. (B) Determination of k_{obs}. Plot of $\ln[(F_t - F_{eq})/(F_0 - F_{eq})]$ versus time for [RRE^{AU}] = ▲, 30 nM; □, 50 nM; ◇, 100 nM; ●, 150 nM; ▼, 200 nM; △, 500 nM. F_{eq} was calculated from the concentration of RRE^{AU} and the K_d of the S1-5-S2·RRE^{AU} complex (68 nM). Each solid line represents the best linear least-squares fit to the data. (C) Determination of k_1 and k_{-1}. Plot of the k_{obs} from part B against [RRE^{AU}]. The open point at [RRE^{AU}] = 0 is from an independent measurement of k_{-1}. The solid line represents the best linear least-squares fit to the data. (D) Competitive analysis. Plot of the effect of S1-5-S2 on the fraction of [^{32}P]S1-5-S2 bound to RRE^{AU} as a function of time. θ = fraction of [^{32}P]S1-5-S2 bound to RRE^{AU}. The solid line represents the simulated time course where $k_2 = 7.8 \times 10^3$ M^{-1} s^{-1} and $k_{-2} = 4 \times 10^{-4}$ s^{-1}. This simulation fit the experimental data with the smallest average residual (2%). The hashed line represents the simulated time course where $k_{-1} = k_{-2} = 9.0 \times 10^{-5}$ s^{-1} (derived from independent measurement of k_{-1} as described in part C) and $k_1 = k_2 = 7.8 \times 10^3$ M^{-1} s^{-1} (derived from direct association kinetic analysis, part C). This simulation fit the experimental data with an average residual of 28%. The dotted line represents the simulated time course where $k_{-1} = k_{-2}$ = 3×10^{-5} s^{-1} and $k_1 = k_2 = 7.8 \times 10^3$ M^{-1} s^{-1}. This simulation fit the experimental data with an average residual of 10%. Residuals for each trial are shown above the corresponding plot.

nM−15 mM competitor in binding buffer. The fraction of [^{32}P]S1-5-S2 bound to RRE^{AU} in the presence of competitor TOP did not change once equilibrium was reached, indicating the absence of slow changes in RRE^{AU} conformation that altered the position of equilibrium.

Rate Constant Determination. Simulated time courses illustrating the time-dependent change in the fraction of [^{32}P]S1-5-S2 bound to RRE^{AU} as a function of competitor concentration were generated by numerical integration of differential equations 2−4 using a Runge−Kutta algorithm.[77] Although the association and dissociation of triplex TOP·RRE^{AU} complexes likely proceed through several discrete steps and intermediates, detection of many of these intermediates is difficult; our experimental assay detects only [^{32}P]S1-5-S2 and [^{32}P]S1-5-S2·RRE^{AU}. We therefore utilized a simple binding model in which the [^{32}P]S1-5-S2·RRE^{AU} and triplex TOP·RRE^{AU} association and dissociation reactions were represented by single second-order and first-order rate constants, respectively. This choice was validated by the observation that the rate constants for [^{32}P]S1-5-S2·RRE^{AU} association and dissociation obtained from direct kinetic experiments were

(77) Margenau, H.; Murphy, G. M. *The Mathematics of Physics and Chemistry*, 2nd ed.; D. Van Nostrand, Co.: Princeton, NJ, 1956.

within a factor of 2 of those obtained from the competitive analysis. Although triplex TOP·RRE^{AU} K_d values calculated from k_2 and k_{-2} were consistently 2.5−6.5-fold lower than those measured by equilibrium methods (Table 1), the former values are more accurate than the latter values, especially for weakly bound TOPs that are not well quantified by gel methods. A 2.5−6.5-fold difference in the values of k_2 and k_{-2} would not alter our mechanistic conclusions.

Results

A series of triplex TOPs (Figure 1) designed to recognize RRE^{AU} (Figure 2B) were synthesized by solid-phase methods. Triplex TOPs S1-1-S4, S1-3-S4, S1-5-S4, and S1-7-S4 contained 5′- and 3′-oligonucleotides designed to interact with discrete regions of RRE^{AU}: the 5′-oligonucleotide complements 8 bases spanning C69−G76 (site 1) to form a duplex, whereas the 3′-oligonucleotide complements the 12 base pairs within stem−loop IIB (site 4) to form a triple helix. Triplex TOPs S1-1-S4[9] and S1-1-S4[6] contained truncated 3′-oligonucleotide sequences, whereas triplex TOPs S1-1-S4^{UC} and S1-1-S4^C contained mutated 3′-oligonucleotide sequences. Oligonucleotides S1 and S1EXT were complementary to only site 1.

Association and Dissociation Kinetics of Triplex TOP·RRE^{AU} Complexes. We used a competitive electrophoretic mobility shift assay[63−65] and a Runge−Kutta algorithm[77] to determine the rate constants for association and dissociation of triplex TOP·RRE^{AU} complexes. This assay quantified the effect of a triplex TOP on the association and dissociation rates of a TOP·RRE^{AU} complex that was stable during gel electrophoresis and whose association and dissociation kinetics were established by direct methods. The TOP·RRE^{AU} complex chosen for this task was S1-5-S2·RRE^{AU},[47] which is stabilized by Watson−Crick interactions at both sites 1 and 2.

The reversible binding reactions monitored in our assay are represented by the following linked equilibria:

$$R\cdot C \underset{k_{-2}}{\overset{k_2[C]}{\rightleftharpoons}} R \underset{k_{-1}}{\overset{k_1[T]}{\rightleftharpoons}} R\cdot T \tag{1}$$
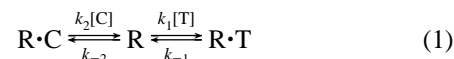
where $K_d^{R\cdot T} = k_{-1}/k_1$, $K_d^{R\cdot C} = k_{-2}/k_2$, and R, C, T, R·T, and R·C represent RRE^{AU}, competitor, [^{32}P]S1-5-S2, [^{32}P]S1-5-S2·RRE^{AU}, and competitor·RRE^{AU}, respectively. k_1 and k_{-1} represent the second-order association and first-order dissociation rate constants of the [^{32}P]S1-5-S2·RRE^{AU} complex; k_2 and k_{-2} represent the second-order association and first-order dissociation constants of the competitor·RRE^{AU} complex.

The kinetics of our competition assay are represented by the following differential rate equations:

$$\frac{d[R]}{dt} = k_{-1}[R\cdot T] + k_{-2}[R\cdot C] - k_1[T][R] - k_2[C][R] \tag{2}$$

$$\frac{d[R\cdot C]}{dt} = k_{-2}[R\cdot C] - k_2[C][R] = -\frac{d[C]}{dt} \tag{3}$$

$$\frac{d[R\cdot T]}{dt} = k_{-1}[R\cdot T] - k_1[T][R] = -\frac{d[T]}{dt} \tag{4}$$

These equations and a Runge−Kutte algorithm[77] were used to simulate the time-dependent change in the concentration of [^{32}P]-S1-5-S2·RRE^{AU} as a function of k_2 and k_{-2}; values for k_1 and k_{-1} were determined independently and fixed at 7.8×10^3 M^{-1} s^{-1} and 4×10^{-4} s^{-1}, respectively. These simulated time courses were compared to the experimental time courses, and k_2 and k_{-2} were varied to optimize the fit. Residuals for trials simulated in this manner ranged between 1.0% and 4.6%.

Association Rate Constants (k_2). The time-dependent effects of S1, S1EXT, and triplex TOPs on the fraction of [^{32}P]-
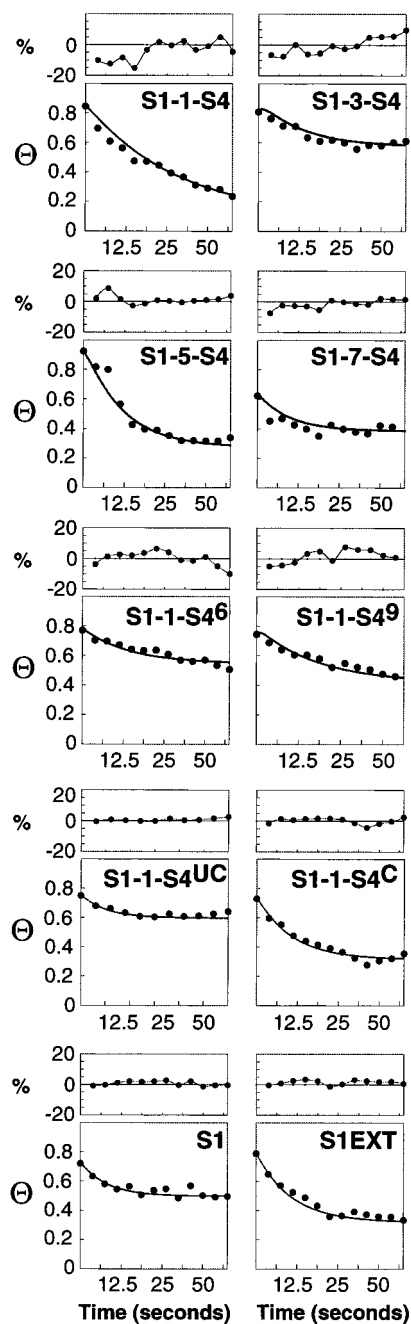
Figure 4. Plots illustrating the effect of triplex TOP or oligonucleotide (●) on θ, the fraction of $[^{32}P]$S1-5-S2 bound to RRE^{AU} as a function of time. The solid line illustrates the simulated best fit to the experimental data. Above each plot is shown the residuals in percent (%). Residuals at each data point were calculated from the equation $(v_e - v_s)/v_s$, where v_e and v_s are the values obtained from experiment and simulation, respectively.[91,92]

S1-5-S2 bound to RRE^{AU} are shown in Figure 4. Superimposed on each plot is the simulated trial that exhibited best fit to the experimental data. Averaged rate constants for all triplex TOP·RRE^{AU} complexes are shown in Table 1. The data show that all triplex TOPs bound RRE^{AU} with similar association kinetics, with k_2 values between $(7.8 \pm 2.0) \times 10^3$ and $(16 \pm 3) \times 10^3$ M^{-1} s^{-1}. For example, the association rate constant was insensitive to the length of the tether separating the 3′- and 5′-oligonucleotides. S1-1-S4, with a single abasic phosphodiester linkage between the 3′- and 5′-oligonucleotides, exhibited an association rate constant that was comparable to those for molecules containing three, five, and seven abasic phosphodi-

ester units. Association rate constants were also insensitive to the length and sequence composition of the 3′-oligonucleotide. S1-1-S4, S1-1-S4^9, S1-1-S4^6, S1-1-S4^C, and S1-1-S4^{UC}, all of which contained a different 3′-oligonucleotide sequences and formed RRE^{AU} complexes with different stabilities, exhibited nearly identical association rate constants. Even an oligonucleotide in which an additional 10 nucleotides were appended to the 3′-end of S1 (S1EXT) exhibited an equivalent association rate constant of $(7.8 \pm 2) \times 10^3$ M^{-1} s^{-1}. Not only were all triplex TOP association rate constants of all triplex TOPs nearly identical to one another, they were also nearly identical to that measured for the association of S1 with RRE^{AU}.

Dissociation Rate Constants (k_{-2}). The rate constants for dissociation of triplex TOP·RRE^{AU} complexes varied by more than 2 orders of magnitude, between $(3 \pm 1) \times 10^{-4}$ and $(540 \pm 200) \times 10^{-4}$ s^{-1}. In general, triplex TOP·RRE^{AU} complexes with the greatest thermodynamic stabilities displayed the lowest dissociation rate constants. S1-1-S4, which formed the most stable RRE^{AU} complex ($K_d = 93 \pm 15$ nM),[62] was characterized by the lowest k_{-2} value ($(3 \pm 1) \times 10^{-4}$ s^{-1}), whereas S1-1-S4^{UC}, which formed the least stable RRE^{AU} complex ($K_d = (30\,900 \pm 3700$ nM) was characterized by the highest k_{-2} value ($(400 \pm 40) \times 10^{-4}$ s^{-1}). The rate constants for dissociation of triplex TOP·RRE^{AU} complexes varied with tether length over a 40-fold range with the following order: S1-1-S4 < S1-3-S4 = S1-5-S4 < S1-7-S4. Dissociation rate constants were also sensitive to the length and sequence of the 3′-oligonucleotide; sequence changes that resulted in mismatched RRE^{AU} complexes significantly increased the dissociation rates of triplex TOP·RRE^{AU} complexes. For example, the dissociation rate of the S1-1-S4^{UC}·RRE^{AU} complex ($k_{-2} = (400 \pm 40) \times 10^{-4}$ s^{-1}), which contained three mismatched Hoogsteen base pairs, was more than 130-fold greater than that of the cognate S1-1-S4·RRE^{AU} complex and approximately the same as that of the S1·RRE^{AU} complex ($k_{-2} = (500 \pm 200) \times 10^{-4}$ s^{-1}). Shortening the 3′-oligonucleotide by three or six nucleotides resulted in 6- or 20-fold increases in k_{-2}.[62] The lifetime of the S1-1-S4·RRE^{AU} complex (3300 s) is comparable to the lifetime of the complex between RRE^{AU} and S1-5-S2 (2500 s), a TOP that binds RRE^{AU} sites 1 and 2 via duplex formation.

Discussion

Each triplex TOP shown in Figure 1 is comprised of two short oligonucleotides joined together with a flexible tether of variable length. We showed previously that triplex TOPs bind RRE^{AU} in a highly specific manner and that both the 3′- and 5′-oligonucleotides hybridize to their prescribed binding sites in the complex.[61,62] Here we used competitive kinetic experiments to investigate the stepwise pathway by which the triplex TOP·RRE^{AU} complex forms. Because there was no simple integrated solution to the differential equations describing the competitive binding reactions, we used numerical integration to simulate the kinetic data. Association rate constants of triplex TOP·RRE^{AU} complexes were comparable to that measured for the S1-5-S2·RRE^{AU} complex and were insensitive to the length and sequence of the 3′-oligonucleotide that mediates triple helix formation. By contrast, dissociation rate constants were sensitive to changes in tether length and the length and sequence of the 3′-oligonucleotide.

Two Pathways for Formation of Triplex TOP·RRE^{AU} Complexes. The assembly of a TOP·RRE^{AU} complex may proceed through two pathways (Figure 5, top). Pathway I is characterized by a first step in which a duplex forms between the 5′-oligonucleotide within each triplex TOP and site 1 of RRE^{AU} and a second step in which a triple helix forms
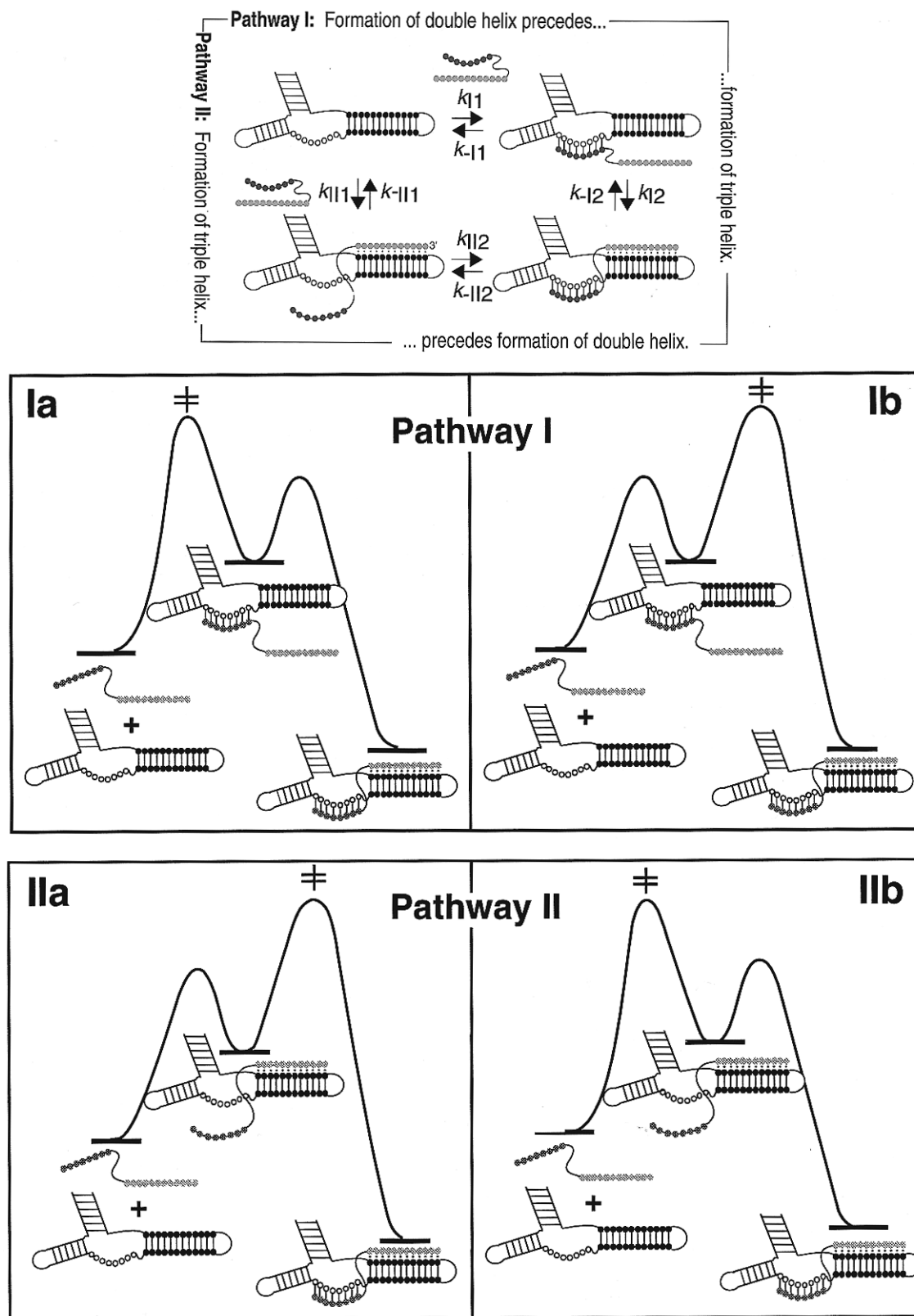
Figure 5. (Top) Two alternative pathways to describe the stepwise formation of a triplex TOP·RRE[AU] complex. In pathway I, formation of a duplex between the 5′-oligonucleotide of the triplex TOP and site 1 of RRE[AU] precedes formation of a triple helix between the 3′-oligonucleotide of the triplex TOP and site 4 of RRE[AU]. In pathway II, formation of the triple helix at site 4 precedes formation of a duplex at site 1. (Bottom) Reaction coordinate diagrams illustrating the free energy along the pathway if (pathways Ia and IIa) formation of the site 1 duplex is rate -limiting (‡) or (pathways Ib and IIb) formation of the site 4 triple helix is rate-limiting (‡).

between the 3′-oligonucleotide and site 4. Pathway II is characterized by a first step in which a triple helix forms between the 3′-oligonucleotide and site 4 of RRE[AU] and a second step in which a duplex forms between the 5′-oligonucleotide and site 1.

Available data on the kinetics of duplex and triple-helix hybridization indicate that neither pathway I or II is unlikely for the assembly of TOP·RRE[AU] complexes. The association of short, unstructured oligonucleotides into duplexes is rapid ($k_{on} = 10^6 - 10^7$ M^{-1} s^{-1})[78] relative to rate constants measured

for triple-helix association ($k_{on} = 10^3$ M^{-1} s^{-1}).[79–82] However, when one of the oligonucleotide partners is structured, duplex association rate constants can decrease by several orders of magnitude into the range observed for triple-helix formation.[42,60,83] S1-5-S2, which disrupts intramolecular Watson—Crick and non-Watson—Crick base pairs within the RRE[84–86] to interact with sites 1 and 2, exhibits an association rate constant of approximately 10^3 M^{-1} s^{-1}. Triplex TOPs also interact with site 1 and therefore must also disrupt these intramolecular base pairs. Since there is little or no information on the effect of RNA structure on triple-helix formation, it is possible that formation of the site 1 duplex could be slower than formation of the site 4 triple helix.

Kinetic Data Provide Evidence for Pathway I. Pathways I and II can each be represented by two energy diagrams that differ in terms of whether duplex formation or triple helix formation is rate-limiting (Figure 5, bottom). In pathways Ia and IIa, formation of a duplex at site 1 is rate-limiting, whereas in pathways Ib and IIb, formation of a triple helix at site 4 is rate-limiting. Our data indicate that all triplex TOPs bind RRE^{AU} with similar second-order rate constants, with values between 7.8×10^3 and 16×10^3 M^{-1} s^{-1}. Not only are all triplex TOP association rate constants similar to one another, they are also similar to the rate constant measured for S1, an oligonucleotide that binds RRE^{AU} at site 1 only. These data indicate that triplex TOP association kinetics are dominated by the rate with which the 5′-oligonucleotide binds site 1 and imply that formation of the site 1 duplex is the rate-limiting step in the binding reaction. This correlation rules out pathways Ib and IIb, in which triple-helix formation is rate-limiting.

Further examination of the kinetic data rules out pathway IIa. The principle of microscopic reversibility demands that a reaction follow the same pathway in the forward and reverse directions.[87] The first dissociative step along pathway IIa involves rate-limiting dissociation of the 5′-oligonucleotide within each TOP from site 1 of RRE^{AU}. Dissociation through this pathway would result in values of k_{-2} that correlated only with sequence within the 5′-oligonucleotide. Instead, triplex TOP dissociation rate constants correlate with sequence within the 3′-oligonucleotide. This analysis rules out pathway IIa and argues in favor of a binding mechanism in which duplex formation at site 1 is rate-limiting and precedes triple-helix formation (pathway Ia).

Association Rate Constants. Because triplex TOP·RRE^{AU} association reactions follow a binding pathway in which duplex formation precedes triple-helix formation and is rate-limiting, values for k_2 reflect the rate with which the 5′-oligonucleotide binds site 1 of RRE^{AU}. These rate constants ($k_2 \sim 10^4$ M^{-1} s^{-1}) are approximately 2 orders of magnitude smaller than those measured for the association of unstructured oligonucleotides into short duplexes ($k_{on} = 10^6–10^7$ M^{-1} s^{-1}).[78,83] It is well known that oligonucleotides can bind structured RNAs with rate constants that are considerably smaller than those found for binding unstructured RNAs.[88–90] The decreases in rate constant are attributable to static or dynamic secondary or tertiary interactions within the RNAs that must be disrupted for binding to occur.[41–43,83] There is considerable evidence that such interactions exist in RRE^{AU}: NMR studies on stem—loop IIB suggest that residues (within site 1) may be stably or transiently base paired.[84–86] Thus, the (relatively) slow association kinetics exhibited by triplex TOPs is most likely the result of structure within RRE^{AU} that must be disrupted for binding to occur.

Dissociation Rate Constants. Because triplex TOPs bind RRE^{AU} through a mechanism in which duplex formation is rate-limiting and precedes triple-helix formation, the values measured for k_{-2} reflect contributions from both duplex and triple-helix dissociation. The dissociation rate constant of the S1-1-S4·RRE^{AU} complex, containing 12 triple-helical base pairs in addition to the site 1 duplex, was comparable to that of a DNA triple helix containing 22 triple-helical base pairs.[79,80] The dissociation rate constants of the S1-1-S4^9·RRE^{AU} and S1-1-S4^6·RRE^{AU} complexes, containing nine and six triple-helical base pairs, respectively, in addition to the site 1 duplex, were comparable to those of a DNA triple helix containing 11 or 13 triple-helical base pairs.[82] Although triplex TOP·RRE^{AU} complexes containing three mismatched Hoogsteen base pairs dissociated more than 100 times faster than analogous complexes lacking mismatches, introduction of a mismatch into a DNA triple helix increases the dissociation rate constant by more than 1000-fold.[80] Presumably, the dissociation rate constants of triplex TOP·RRE^{AU} complexes are less sensitive to mismatches because dissociation of both the duplex and the triple helix contributes to the dissociation rate constant k_{-2}.

Conclusions

Here we employed kinetic methods to analyze the interactions between triplex tethered oligonucleotide probes and a modified version of the Rev response element, RRE^{AU}. We find that the rate constants for association of triplex TOP·RRE^{AU} complexes are independent of the structure and stability of the triple helix, whereas the rate constants for dissociation are not. These findings allow us to propose a binding pathway in which duplex formation is rate-limiting and precedes triple-helix formation (pathway 1a in Figure 5). This conclusion implies that the bimolecular reaction between a triplex TOP and RRE^{AU} site 4 (the first step of pathway IIa) must proceed more slowly than the observed association rate constant, 10^4 M^{-1} s^{-1}. Since this rate constant also represents that observed for forming model triple helices, our results imply that triple-helix association reactions are hindered in the context of the structured RREV^{AU} target. Triplex TOPs are unique in that they appear to benefit from the thermodynamic stability of the triple helix as well as the (comparatively) rapid rate constants for duplex formation.

(78) Cantor, C. R.; Schimmel, P. R. *The Behavior of Biological Macromolecules*; Freeman: New York, 1971.
(79) Maher, L. J.; Dervan, P. B.; Wold, B. *Biochemistry* **1990**, *29*, 8820.
(80) Rougee, M. F. B.; Mergny, J. L.; Barcelo, F.; Giovannangeli, C.; Garestier, T.; Helene, C. *Biochemistry* **1992**, *31*, 9269.
(81) Bates, P. J. D.; Kumar, S.; Jenkins, T. C.; Laughton, C. A.; Neidle, S. *Nucleic Acids Res.* **1995**, *23*, 3627.
(82) Yang, M.; Ghosh, S.; Millar, D. P. *Biochemistry* **1994**, *33*, 15329.
(83) Lima, W. F.; Monia, B. P.; Ecker, D. J.; Freier, S. M. *Biochemistry* **1992**, *31*, 12055.
(84) Peterson, R. D.; Bartel, D. P.; Szostak, J. W.; Horvath, S. J.; Feigon, J. *Biochemistry* **1994**, *33*, 5357.
(85) Battiste, J. L.; Tan, R.; Frankel, A. D.; Williamson, J. R. *Biochemistry* **1994**, *33*, 2741.
(86) Battiste, J. L.; Mao, H.; Rao, N. S.; Tan, R.; Muhandiram, D. R.; Kay, L. E.; Frankel, A. D.; Williamson, J. R. *Science* **1996**, *273*, 1547.
(87) Jencks, W. P. *Catalysis in Chemistry and Enzymology*; McGraw-Hill: New York, 1969.

(88) Studier, F. W. *J. Mol. Biol.* **1969**, *41*, 199.
(89) Straus, N. A.; Bonner, T. I. *Biochim. Biophys. Acta* **1971**, *277*, 87.
(90) Gamper, H. B.; Cimino, G. C.; Hearst, J. E. *J. Mol. Biol.* **1987**, *197*, 349.
(91) Strike, P. W. *Statistical Methods in Laboratory Medicine*; Butterworth-Heinemann: Boston, 1991.
(92) Cook, R. D.; Weisberg, S. *Residuals and Influence in Regression Analysis*; Chapman & Hall: London, 1982.